REVIEW

National Science Review
3: 174–188, 2016
doi: 10.1093/nsr/nww018
Advance access publication 21 April 2016

PHYSICS

Special Topic: Cold Atoms

Heteronuclear Efimov resonances in ultracold quantum gases

Juris Ulmanis[1], Stephan Häfner[1], Eva D. Kuhnle[1] and Matthias Weidemüller[1,2,*]

[1]Physikalisches Institut, Universität Heidelberg, Im Neuenheimer Feld 226, 69120 Heidelberg, Germany and [2]Hefei National Laboratory for Physical Sciences at the Microscale and Department of Modern Physics, and CAS Center for Excellence and Synergetic Innovation Center in Quantum Information and Quantum Physics, University of Science and Technology of China, Hefei 230026, China

*Corresponding author. Email: weidemueller@uni-heidelberg.de

Received 14 January 2016; **Revised** 17 March 2016; **Accepted** 18 March 2016

ABSTRACT

The Efimov scenario is a universal three-body effect addressing many areas of modern quantum physics. It plays an important role in the transition between few- and many-body physics and has enabled important breakthroughs in the understanding of the universal few-body theory. We review the basic concepts of the Efimov scenario with specific emphasis on the similarities and differences between homonuclear and heteronuclear systems. In the latter scenario, the existence of a second, independently tunable interaction parameter enables novel few-body phenomena that are universal and have no counterexamples in the homonuclear case. We discuss recent experimental approaches using ultracold atomic gases with magnetically tunable interactions and elucidate the role of short-range interactions in the emergence of universal and non-universal behavior.

Keywords: Efimov resonances, few-body physics, Feshbach resonances, ultracold atoms, resonant scattering

INTRODUCTION

The binding of three pairwise resonantly interacting particles into three-body states, today often termed the Efimov effect, is a prime example for the emergence of universality in quantum few-body systems [1–3]. It is characterized by its extraordinary properties, one of which is the existence of an infinite number of bound three-body states (Efimov states) even when the underlying two-body interactions are not sufficiently strong to support a single bound two-body state. Therefore, exactly as the three Borromean rings would fall apart, if only a single one was removed, the whole three-body system disintegrates as soon as one particle is missing. The Efimov trimer energies and their overall spatial extent are following a geometrical progression, a discrete scaling law, that is governed solely by the quantum statistics, masses and number of resonant pairwise interactions.

The important role of the Efimov effect in modern quantum mechanics is based on its predicted universal behavior for three-body systems with different microscopic details. The interaction between a pair of particles in the low-energy limit is described by the two-body *s*-wave scattering length *a*. Whenever its magnitude significantly exceeds the characteristic range of interparticle interactions r_0, the two-body wavefunction greatly extends into the classically forbidden region, where the pairwise potentials cease to exist. Thus, the specific details of the individual potential become irrelevant, giving rise to universal bound state energies close to the scattering threshold and halo wavefunctions, both of which are governed by the sole parameter *a*—a single length scale that characterizes the entire system. The two-body universality directly transfers to the three-body realm, where it takes the form of the Efimov effect. It manifests for any system resonantly interacting via short-range forces alike, independent if it is the van der Waals force between atoms or the strong force between nucleons [4–7].

The Efimov effect and universal three-body problems can often be found in various areas of modern physics. Triatomic helium, $^4He_3$, was the very first system, for which the existence of Efimov states was suggested [8,9]. Because of the accidental finetuning by nature, the scattering length between two identical ^{4}He atoms is $a = 90.4$ Å (1 Å= 0.1 nm), while the extension of the van der Waals force is only around 5 Å [10]. Thus, the helium potential supports a single two-body state, and two bound three-body states, of which the higher lying one is located well in the Efimovian regime. Recently, the excited $^4He_3$ was produced in a seminal experiment [11], excellently aligning with the long-established predictions from the few-body theories and previous experiments. Observation of a universal $^4He_4$ tetramer might also be within reach [12].

Halo nuclei are the most prototypical examples of universality in nuclear physics [13–16]. The nuclei of ^{11}Be or ^{6}He and ^{11}Li, where a compact core of nucleons is surrounded by one or two loosely bound neutrons, respectively, are major archetypes for studies of universal properties in two- and three-body systems that are composed of different particles. The existence of Efimov trimer states has been speculated in many isotopes [15,17,18], most recently in ^{22}C [19], the heaviest observed Borromean nucleus so far [20], and ^{60}Ca [21], in this way challenging the experimentalists and the present understanding of nuclear behavior in extreme conditions along the neutron drip line [22]. Studies of these and similar systems can have deep consequences not only for nuclear physics and astronomy, but also the potential to reveal new phenomena and three-body effects that are applicable in other fields as well.

The exploration of three-body problems and the Efimov scenario in ultracold gases has initially been motivated by two interconnected aspects. First, the three-body recombination in dilute atomic gases was seen as undesirable loss mechanism limiting the lifetime and stability of these strongly interacting quantum systems. Thus, understanding such processes and finding handles to control them was considered necessary in order to produce large and long-lived many-body systems. Second, it was realized that Feshbach resonances [23,24], which enable the tuning of scattering length by simply exposing the gas of ultracold atoms to an external magnetic field, can be employed to manipulate the two-body interaction from infinite repulsion to attraction, thus, offering unique opportunities in the research of universal and Efimov physics. With the help of such scattering resonances, the interactions governing the quantum behavior of ultracold systems could be manipulated in a well-controlled manner, therefore, providing experimentalists not only with well-suited experimental observables for testing few-body scenarios, but also a control knob for exploring strongly interacting regimes.

The experimental realization of Efimov states and with them related physics is challenging, which is also the reason why they were first demonstrated in ultracold atoms only in 2006 [25], more than thirty years after the initial proposal. This seminal achievement, where an Efimov state was observed at a crossing with the three-body dissociation threshold for scattering length $a_-^{(0)}$, reminiscent to level crossing spectroscopy from atomic and molecular physics, established measurements of three-body recombination rates [26–28] as a standard tool for probing the Efimov scenario. Only afterwards more direct methods such as trimer photoassociation with radio-frequency photons [29–31] or formation of He trimers in a supersonic expansion [11], were able to investigate the three-body energy spectra beyond zero energy. Several excellent reviews [5,7,32–37] extensively cover most of these topics for ultracold gases.

An even richer form of the Efimov scenario emerges in a three-body system that is composed of two identical bosonic particles and a third one that is different. In such heteronuclear systems, only ^{40}K-^{87}Rb [38,39], ^{41}K-^{87}Rb [40,41], ^{7}Li-^{87}Rb [42] and ^{6}Li-^{133}Cs [43–46] mixtures have been investigated so far, with varying success [38,47,48]. Except for the latter, only ground state Efimov resonances ($a < 0$) have been observed, since the large scaling factors and high temperatures make the observation of excited features complicated. Direct investigation of the universal scaling has been possible only for the Li-Cs mixture, where three consecutive features have been observed that display both universal and non-universal behavior.

A wealth of few- and many-body topics, to which the Efimov scenario is one of the most fundamental building blocks, is reflected in many recent reviews in this area [5–7,32–37,49]. We will focus on the three-body system of two indistinguishable bosons and one distinguishable particle, as this combination of particles, while in some aspects similar to three alike bosons, represents the most simple heteronuclear system at the next level of complexity. This extension already leads to rich three-body physics that contain phenomena, which have no counterexamples in the homonuclear case. Furthermore, recent experiments in ultracold gases have exclusively investigated exactly such systems, partly still restricted by the limited knowledge and technological means in fully controlling interactions and all degrees of freedom in quantum systems that are consisting of three very different particles. In view of broad coverage, this review shortly reiterates the fundamental principles and discusses experimental signatures of three-body scenarios that are basic requirements in the quest towards understanding the heteronuclear Efimov effect. We also address further intriguing

Table 1. Dispersion coefficients C_6 (taken from [50]), van der Waals radii r_{vdW} and energies E_{vdW}, and thermal de-Broglie wavelengths Λ_{dB} for temperatures of 1 μK and 100 nK for a few of typical alkaline metal mixtures.

System	C_6 (au)	r_{vdW} (a_0)	E_{vdW} (MHz)	Λ_{dB} (a_0) (1 μK)	Λ_{dB} (a_0) (100 nK)
K-Rb	4274	72	13	6000	20000
Li-Rb	2545	44	143	13000	41000
Li-Cs	3065	45	156	14000	43000

questions, for example, the transition between universal and non-universal physics, where individual details of interaction potentials matter, and discuss experiments on mixtures of ultracold quantum gases, that during the last decade have been the major test bed for exploring the exciting few-body world.

TWO-BODY INTERACTIONS AND UNIVERSALITY

Two-body scattering at low energies

The scattering theory for two particles, interacting with a pairwise potential $V(\mathbf{r})$, can be found in standard quantum mechanics text books [51]. The Schrödinger equation is solved for an incoming plane wave with wave number k and a scattered wave in the partial wave expansion. If the potential is isotropic and for low energies, where the de Broglie wavelength $\Lambda_{dB} = 2\pi/k$ is larger than the range r_0 of the potential, only the zero angular momentum ($l = 0$) partial wave is important (s-wave scattering). The scattering phase shift $\delta_0(k)$ between the incoming and scattered wave comprises the relevant effect of the interaction potential on the collision. In the zero-energy limit ($k \to 0$), $\delta_0(k)$ can be expanded in powers of k^2 in the so-called effective range expansion

$$k \cot \delta_0(k) = -\frac{1}{a} + \frac{1}{2} r_e k^2, \qquad (1)$$

where a is the scattering length and r_e the effective range. The collision is indistinguishable from one that is based on a contact interaction for low particle momenta, where $r_e k < 1$ and the scattering process can be solely described by the s-wave scattering length a.

The interaction between two atoms is given by the Born–Oppenheimer (BO) molecular potentials. For distances that exceed the size of the individual electron clouds of each atom, the potential is attractive and displays the van der Waals (vdW) form

$$V(r) = -\frac{C_6}{r^6}, \qquad (2)$$

where r is the distance between the two nuclei, and the dispersion coefficient C_6 depends on the details of the electronic configurations and is often obtained from either *ab initio* calculations (see for example [50,52,53]), photoassociation [54] or Feshbach spectroscopy [23,24].

Natural energy and length scales in ultracold atom scattering

The van der Waals behavior of the molecular interaction potential allows one to introduce the characteristic length and energy scales r_{vdW} and E_{vdW}, respectively, which read [23]

$$r_{vdW} = \frac{1}{2}\left(\frac{2\mu C_6}{\hbar^2}\right)^{1/4} \qquad (3)$$

and

$$E_{vdW} = \frac{\hbar^2}{2\mu r_{vdW}^2}, \qquad (4)$$

where μ is the two-body reduced mass and $\hbar$ the reduced Planck constant. For ultracold binary collisions of neutral atoms, the vdW scales determine the threshold between the short-range ($r < r_{vdW}$) and long-range ($r > r_{vdW}$) behavior of the two-body potential. In the case of a general two-body system, this parameter is typically denoted by r_0, since other forces may create the short-range potentials. The short-range region is dominated by fast oscillations of the scattering wavefunction because the local wavenumber becomes large in comparison to the asymptotic one. In the long-range region, the wavefunction approaches its asymptotic form that is governed by the de Broglie wavelength of the ultracold collision, while a bound wavefunction decays exponentially. Any bound two-body state will exhibit spatial extension on the order of or smaller than r_0, with the only exception of the last s-wave bound state for the case of the universal halo dimer, for which $a > r_0$ [23]. We have summarized some of the natural length scales for a few of experimentally employed atom mixtures in Table 1.

Tuning the interactions via Feshbach resonances

While in nuclear, atomic or molecular systems the scattering length is fixed by the details of the

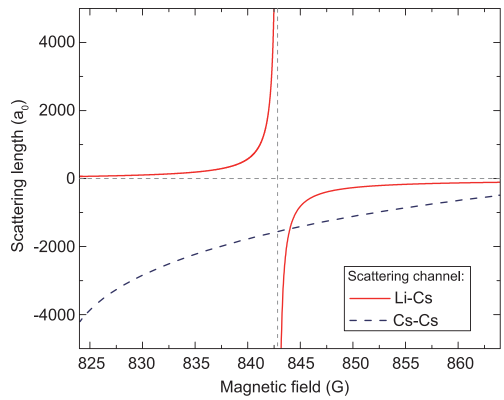

Figure 1. Inter- and intraspecies scattering lengths a and $\bar{a}$ for Li-Cs (red solid line, data taken from [45]) and Cs-Cs (blue dashed line, data taken from [55]) collisions, respectively, in their energetically lowest magnetic spin states.

interaction potential, both its sign and size can be tuned in ultracold atomic gases by magnetic Feshbach resonances [23]. Therefore, we consider two molecular potentials: the open or entrance channel and the closed channel. If the closed channel supports a bound state and the two molecular potentials have different magnetic moments, the energy difference of the bound state and the scattering state in the entrance channel can be tuned to zero. Even a small coupling leads to a large mixing of the two states and the scattering length diverges. The dependence of a on the magnetic field B is given by the typical dispersion relation [23,56]

$$a(B) = a_{\mathrm{bg}}\left(1 - \frac{\Delta}{B - B_0}\right), \tag{5}$$

where a_{bg} is the background scattering length, Δ is the width of the resonance and B_0 defines the pole of the Feshbach resonance. This way the scattering length can be tuned from $-\infty$ to ∞. This behavior is shown in Fig. 1 for the cases of Li-Cs and Cs-Cs. Due to different molecular potentials, the specific parameters of a Feshbach resonance depend a lot on the individual two-atom system [23]. This leads to a distinct scattering length landscape for each combination and overlapping Feshbach resonances.

Since the scattering length a is an essential quantity in ultracold collision processes, knowledge of its magnetic field dependence is crucial. As the three-body loss coefficient in the vicinity of Feshbach resonances depends on the scattering length, magnetic-field-dependent loss measurements can be used to quantify the relation $a(B)$. The combination of atom loss spectroscopy and various theoretical models can be used to obtain an excellent description of the general resonance spectrum and the resonance parameters [23,57]. At the same time, for large scattering lengths, it is challenging to quantitatively connect an increase in three-body loss with an increasing scattering length. In this regime asymmetric broadening or shifts of the loss maximum with respect to the resonance position can be observed [58–63] (see also Fig. 2), and a reliable extraction of resonance parameters is complicated.

In order to unambiguously determine the Feshbach resonance parameters, it is favorable to study the magnetic field dependence of the binding energy of the least-bound molecular state [23,24,64]. Since a Feshbach resonance intrinsically originates from the coupling of the scattering channel to such a molecular state, its binding energy E_b in the vicinity of the resonance is connected to the scattering length through the relation $E_b \propto a^{-2}$ [23,65]. Thus, a measurement of the function $E_b(B)$ gives more direct access to the mapping $a(B)$ that is shown in Fig. 2 for a Li-Cs Feshbach resonance.

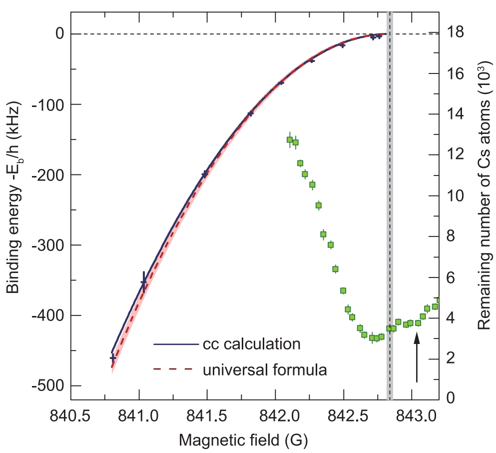

Figure 2. Dimer binding energy versus magnetic field for the 843 G Li-Cs Feshbach resonance. The experimental data (blue crosses) are compared to the universal formula $E_b = \hbar^2/2\mu a^2$ (red dashed line) and to a coupled channels calculation (blue solid line). The gray dashed line and the shaded area represent the resonance position and its uncertainty. The green squares show the remaining number of Cs atoms from atom loss spectroscopy, and the arrow indicates the position of an Efimov resonance. Reprinted from [45], licensed under CC BY 3.0.

THE EFIMOV SCENARIO

The basic morphology of the Efimov scenario as a function of scattering length for a general three-body system, including the homonuclear as well as the heteronuclear case, is illustrated in Fig. 3. The Efimov energy diagram consists of three major parts. Above the three-body dissociation threshold ($E > 0$), the particles are unbound and their energy

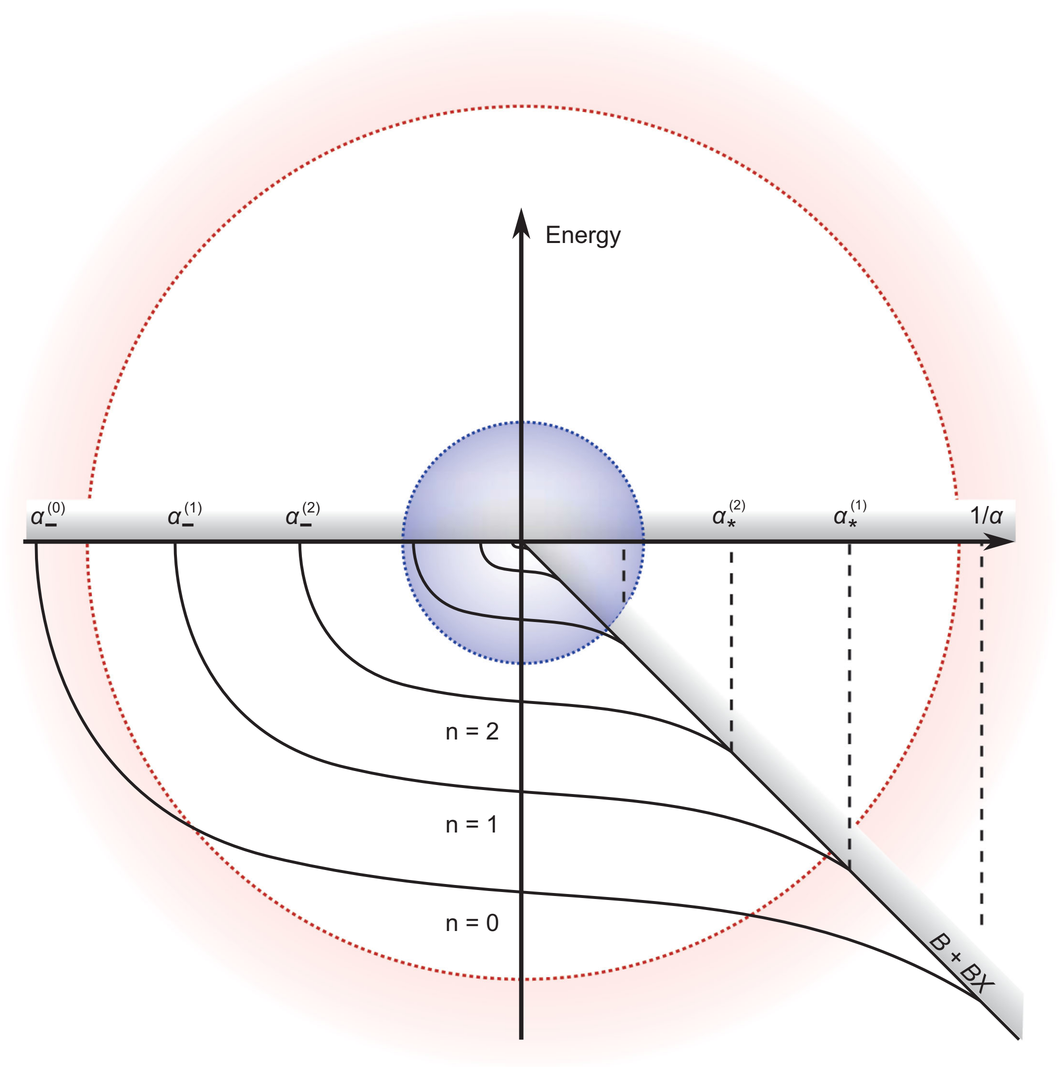

Figure 3. Sketch of the heteronuclear Efimov scenario for two identical bosons B and one distinguishable particle X. If the particle X is identical to B one recovers the homonuclear case. A similar energy level structure manifests for any other system where the Efimov effect exists. Shown are a few of the deepest bound three-body energy levels as a function of the interspecies scattering length a between particles B and X, while the intraspecies scattering length $\bar{a}$ between bosons B is resonant ($\bar{a} \to \infty$). Atom-dimer scattering threshold is given by $B + BX$. The window of universality ($\Lambda_{\rm dB} \gg |a| \gg \max(r_0, \bar{r}_0)$) is located between the temperature (blue shaded area) and short-range (red shaded area) dominated regimes, which are characterized by the de Broglie wavelength $\Lambda_{\rm dB}$ and the additional length scales r_0 and $\bar{r}_0$ of the two-body interaction, respectively.

spectrum is continuous and largely independent of the magnetic field or the scattering length. Below the three-body dissociation threshold ($E < 0$), the system behaves differently depending on the sign of the scattering length. For $a > 0$ the system supports a weakly bound two-body state, the universal dimer state, while for $a < 0$ there are no two-body bound states present. The three-body bound states that connect the atom-dimer threshold at $a > 0$ with the three-body dissociation threshold at $a < 0$ are the Efimov states. For systems consisting of atoms, deeply bound two-body states exist independently of the scattering length, however, they are not required and they are not part of the Efimov effect. (An exception is the $^4He_2$ interaction potential, which supports only a single bound dimer state, close to the universal regime.)

The Efimov states exhibit several remarkable properties, one of them being the discrete scaling symmetry. They are self-similar under rescaling of all length scales by a discrete factor λ. Their energy spectrum at the scattering resonance E_n, the positions $a_-^{(n)}$ and $a_*^{(n)}$ at which each trimer state crosses the three-body dissociation threshold and the

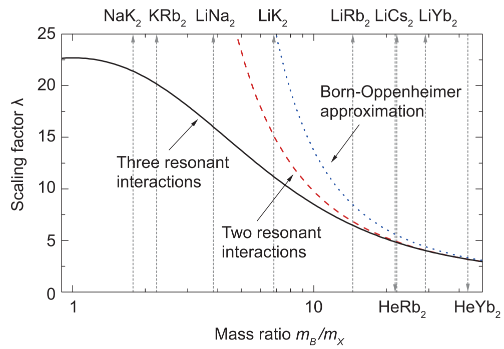

Figure 4. Efimov scaling factor as a function of the mass ratio for a system of two identical bosons B with mass m_B and one distinguishable particle X with mass m_X for three (black solid line) and two (red dashed line) resonant interactions, and in BO approximation (blue dotted line). Vertical dashed lines show mass-ratios for a selection of experimentally employed heteronuclear mixtures.

atom-dimer threshold, respectively (see Fig. 3), are described by the discrete scaling laws

$$
\begin{aligned}
E_{n+1} &= \lambda^{-2} E_n, \\
a_-^{(n+1)} &= \lambda a_-^{(n)}, \\
a_*^{(n+1)} &= \lambda a_*^{(n)},
\end{aligned}
\tag{6}
$$

where the scaling factor $\lambda = e^{\pi/s_0}$ is governed by a single dimensionless parameter s_0, and n is the index of the Efimov state (for the ground state $n = 0$). This is a direct consequence of an attractive $\propto -(s_0^2 + 1/4)/R^2$ hyperspherical potential, where R is the hyperradius that can be defined as the quadratic mean of pairwise separations between the three particles [5]. It can support an infinite number of quantized energy levels [66–68], which is also the reason behind the infinite geometrical progression of the three-body bound states.

In realistic systems and systems with two distinguishable and finite scattering lengths, the scaling symmetry is not exact, since the hyperspherical potential does not perfectly follow the $\propto - R^{-2}$ law, and the scaling factor λ_n depends on the Efimov period n. As one approaches higher excited states, such that $a \to \infty$, and the length scales of a and $\bar{a}$ can be separated, the ideal Efimov scenario is recovered with $\lambda = \lambda_n = \lambda_{n+1}$. The discrete scaling symmetry in the resonant limit implies that different characteristic quantities E_n, $a_-^{(n)}$, and $a_*^{(n)}$ are also related to each other by universal constants [5,37].

Scaling factor

For a general three-body system the parameter s_0 is determined by the mass ratio, number of resonant interactions, and the quantum statistics of the particles, as the correct symmetry of the scattering wavefunction needs to be imposed. Once these properties are known, the parameter s_0 determines the entire structure of the Efimov spectrum. Different situations were already discussed by Amado and Noble [69] and Efimov himself [1–3,70]. In fact, not every combination of three particles results in the Efimov effect, however, most of the traditional three-body systems in this respect are extensively reviewed in [5,36].

For the most recent experiments, a general system *BBX*, which consists of two identical bosons *B* and a third distinguishable particle *X* with masses m_B and m_X, respectively, is of particular interest. The corresponding scaling factors are shown in Fig. 4 as a function of the mass ratio m_B/m_X and given in Table 2 for typical mixtures. As the mass ratio is increased the scaling factor decreases, leading to a denser Efimov energy spectrum. This is beneficial for the experimental observation of several consecutive Efimov resonances [47,71]. A series of denser lying features can be observed at higher temperatures, and the requirements for the tunability of the scattering length, for example, the required magnetic field stability and width of the employed Feshbach resonance, can be relaxed in comparison to the homonuclear case. Exactly, this

Table 2. Universal scaling factors for different mass ratios m_B/m_X. The scaling factors λ, λ^*, and λ^{BO} are given for two, three resonant interactions, and the BO approximation, respectively.

System	m_B/m_X	λ	λ^*	λ^{BO}
^{87}Rb-$^{41}K_2$	0.47	350×10^3	21.3	–
BBX	1	1986	22.7	–
^{23}Na-$^{39}K_2$	1.69	251	21.6	18×10^3
^{40}K-$^{87}Rb_2$	2.17	123	20.3	1641
^{7}Li-$^{23}Na_2$	3.28	36.3	16.0	111
^{6}Li-$^{39}K_2$	6.48	16.2	11.6	28.9
^{7}Li-$^{87}Rb_2$	12.4	7.89	7.26	10.2
^{4}He-$^{87}Rb_2$	21.7	4.94	4.86	5.60
^{6}Li-$^{133}Cs_2$	22.1	4.88	4.80	5.52
^{6}Li-$^{174}Yb_2$	28.9	4.05	4.02	4.41

property enabled the first observation of three consecutive Efimov features via recombination rate measurements [46].

Two approaches in calculating λ are the Faddeev equations [72] and Efimov's original work [1,2,70] that are reviewed in [5,36], respectively. The scaling factors can also be calculated from the BO approximation, which takes advantage of the large mass imbalance [73]. While it delivers a much more intuitive picture, in the simplest implementation (see for example [37,74]) it does not distinguish between two and three resonant interactions, and the scaling factors strongly deviate from the more precise models for small mass ratios. Nevertheless, for larger mass ratios the BO approximation is excellent for estimating characteristic scaling factors and is essentially exact in the limit $m_B/m_X \to \infty$.

Depending on the number of resonant interactions in the system, the scaling exponent acquires one of two distinct values: s_0 (corresponding to two resonant interactions) or s_0^* (corresponding to three resonant interactions). The difference between them increases as the mass ratio is decreased, suggesting that the scaling factor in systems with intermediate mass imbalance, for example, LiK_2 or $LiNa_2$, can take a broad range of values depending on the exact magnitude of the interaction strength between the two like particles. Furthermore, the limit $R/a \to \infty$ is not strictly justified anymore, which leads to deviations from the $\propto - R^{-2}$ behavior of the hyperspherical potential and, consequently, modified trimer energy and recombination resonance spectra, deviating from the discrete scale invariance. This, however, has not been actively investigated yet, since the scaling factor itself is large, and therefore the experimental observation of a series of Efimov states is challenging. It might be feasible in the most recent experiments with drastically reduced scaling factors [42–44].

Intraspecies scattering length

The second scattering length that is crucial in a complete description of the heteronuclear Efimov effect is the intraspecies scattering length $\bar{a}$ between the two identical bosons B. The three-body energy spectrum as a function of $\bar{a}$ also contains an infinite series of three-body states that are log-periodically spaced with the respective scaling factor (see Fig. 5). Depending on the number of resonant interactions (two, if $a \to \infty$ and $\bar{a} = 0$, or three, if $a, \bar{a} \to \infty$), two limiting regimes with different scaling factors can be distinguished [5,75]. General considerations suggest that the interaction strength that separates them can be associated with the characteristic length scale $\bar{r}_0$ of the two-body interaction between the alike pair of particles. In Fig. 5, this transition is represented by a step-like behavior around the value $1/\bar{r}_0$. Despite the fact that the

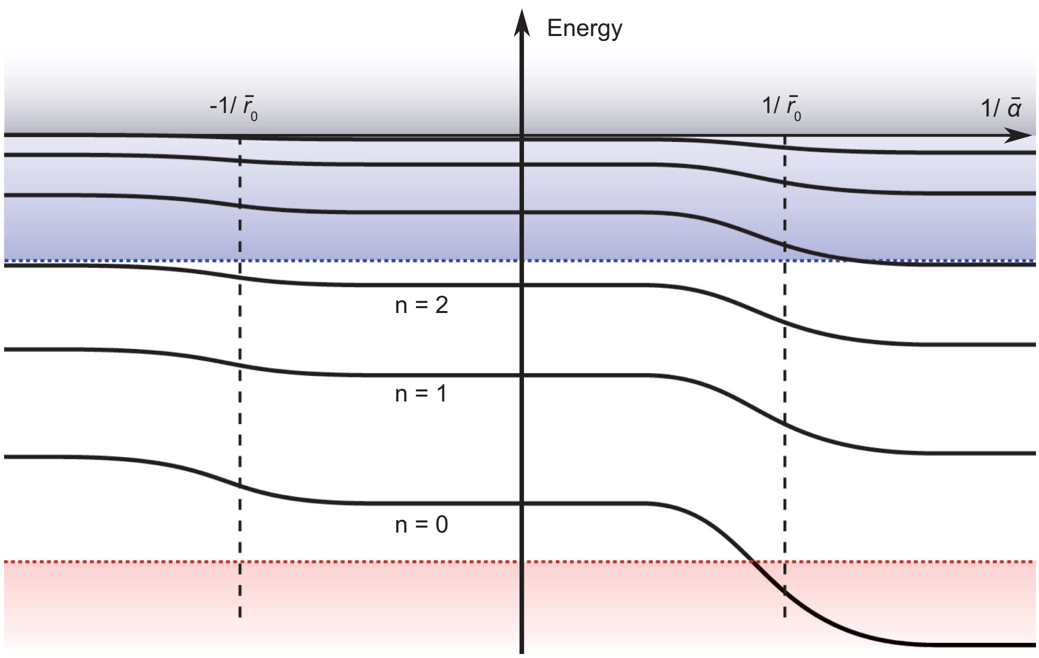

Figure 5. Sketch of a few of the deepest bound energy levels as a function of the intraspecies scattering length $\bar{a}$ between bosons B while $a \to \infty$. The characteristic length scale of the two-body interaction between the bosons is shown by $\bar{r}_0$. The region between the blue and red shaded areas is the window of universality as in Fig. 3.

transition between these regimes is an intriguing topic [76], it has not been studied in detail so far. Systematic investigation of the heteronuclear Efimov scenario, especially its dependence on the interspecies scattering length $\bar{a}$, is an interesting future research topic.

THREE-BODY PARAMETER AND VAN DER WAALS INTERACTIONS

For vanishing particle separations a pure $\propto -R^{-2}$ potential changes so fast that the ground state energy of the trimer level spectrum diverges, reminiscent of the Thomas effect [77], and well-known in quantum physics as 'fall to the center' [66]. This singularity originates from the assumption that the pairwise interactions can be described by the contact interaction as discussed in the second section. To regularize the diverging potential and obtain a well defined energy of the ground state, a cut-off in either real or momentum space can be introduced [5]. This so-called three-body parameter (3BP), in either of its various forms fixes the energies of an Efimov progression and is chosen such that it reproduces the experimental observables, for example, E_0, $a_-^{(0)}$ or $a_*^{(0)}$. In this way, the usual complexity of a real three-body potential is extremely simplified, especially since three-body forces may enter the short-range potential in a nontrivial manner [78,79].

The exact dependence of the three-body parameter on the details of the individual short-range pairwise potentials has been a longstanding open question, since in zero-range theory this information is lost. In spite of early theoretical assumptions suggesting a 3BP that critically depends on the specific details of the short-range two- and three-body interactions [78], for homonuclear atom systems it was found to be approximately constant, if expressed in units of r_{vdW} [80–82]. This apparent contradiction was promptly explained by a universal effective barrier that emerges in the three-body potential and prevents the three particles from simultaneously approaching each other closer than $\sim 2r_{\mathrm{vdW}}$ [83,84]. Thus, the scattering wavefunction is expelled from short interparticle distances, giving rise to approximately universal three-body states that are only possible for large enough separations. In fact, molecular van der Waals tails that are on the order of these length scales are responsible for the formation of such a barrier. Based on this idea for neutral atoms, further universality classes for potentials with scaling other than r^{-6} have been proposed, with relevance not only for ultracold atoms, but also for nuclear and solid-state physics [85]. The surprising indifference of low-energy three-body scattering observables on the details of three-body forces has also motivated the introduction of a general description for few-atom systems that is solely based on pairwise van der Waals forces and hence called van der Waals universality [86].

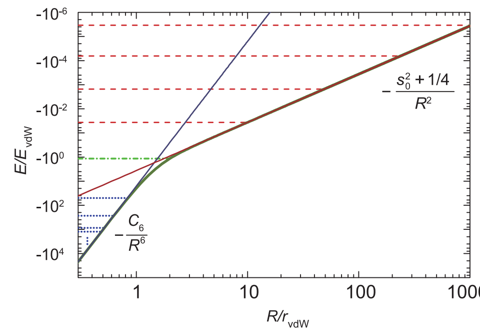

Figure 6. Sketch of the long-range BO potential (green solid line) between two heavy bosons B as a function of their separation R in the presence of a light atom X. The long-range part (red solid line) with scaling $\propto -R^{-2}$ is originating from the interaction with X, while the short-range part (blue solid line) is dominated by the B–B molecular van der Waals tail. The resulting bound state energies are shown as horizontal lines in the vdW (blue dotted), Efimovian (red dashed), and transition (green dot-dashed) dominated regimes. In this figure, $a \to \infty$, $\bar{a} \to \infty$, and $s_0 = 1.98277$.

The 3BP in heteronuclear atomic systems is also expected to be universal with respect to van der Waals forces, although the microscopic mechanism giving rise to the regularization at short distances depends on the mass ratio [76]. For 'Efimov favored' systems consisting of two heavy and one light atom with $s_0 > 1$, the universality of the 3BP is intuitively understood in the BO approximation. Here, it is a universal property of the atomic van der Waals interaction between the heavy atoms that allows one to analytically determine the 3BP in the limit $m_{\mathrm{B}}/m_{\mathrm{X}} \to \infty$. A sketch of such a minimalistic regularization in the BO picture is shown in Fig. 6. In contrast, for 'Efimov-unfavored' systems, containing two light and one heavy atom, the BO picture becomes invalid. In these systems, the 3BP universality originates from a universal three-body repulsion in the range of the van der Waals radius, which, reminiscent of the homonuclear case, shields the three atoms from probing the complicated interactions at a shorter range. Irrespective of the microscopic origin, these interactions govern the energy of the ground Efimov state and fix the absolute position of Efimov trimer progression.

The simplification through the 3BP holds extremely well as long as the transition between the Efimov and van der Waals physics dominated ranges is rapid enough, such that the contributions of the short-range potential to the Efimovian one are negligible. This is mostly the case for homonuclear systems, where the ground state Efimov resonances are typically found at atom separations that are well in the universal regime [81], and the scaling factors are large. In these systems, the first Efimov resonance (the ground state) is found at a scattering length $a_-^{(0)} \sim -9r_{\mathrm{vdW}}$ such that the wavefunction of the trimer predominantly probes the universal parts of the underlying hyperradial potentials.

In contrast, for heteronuclear systems the first Efimov resonance was observed at $a_-^{(0)} \sim -3r_{\mathrm{vdW}}$ [43–45], hence, in combination with reduced scaling factors, the influence of the remaining van der Waals interaction can be expected to be significantly larger and modifications to the Efimov trimer spectra more pronounced (see Fig. 6). As the energy of an Efimov state approaches the energy scale of van der Waals interaction, it is natural to expect modifications to the pure R^{-2} potential, which can result in a scaling factor that depends on the Efimov period. The exact mechanism of this transition between the short- and long-range dominated parts is a current research topic that is being actively investigated [87–93].

UNIVERSAL SCALING LAWS OF SCATTERING RESONANCES

One of the most straightforward and widely used methods in extracting information about three-body physics from an ultracold sample of atoms relies on the measurements of elastic and inelastic few-body collision rates. Since magnetic field can be mapped onto the scattering length, the time evolution of the number of trapped atoms for a given interaction strength delivers direct information about the occurring few-body processes. For atoms in their lowest internal energy state, inelastic two-body collisions are suppressed due to energy conservation, and therefore, they do not contribute to atom loss from the trap. The dominating loss mechanism is three-body scattering, which also crucially depends on the Efimov effect. Each three-body collision may result in inelastic recombination, where two atoms form a bound molecule, and the binding energy is converted into kinetic energy that is redistributed between the dimer and the third atom. Since the trapping potential is typically much lower than the released energy, each such event results in a loss of the products from the trap, which can be easily observed by standard absorption imaging techniques [94]. Efimov resonances then emerge as enhanced inelastic three-body loss features in the recombination spectrum [26–28].

The inelastic three-body recombination in ultracold gases is typically described by the rate coefficient L_3 that depends on the mass ratio of the three particles, the relative magnitude of the pairwise scattering lengths, and quantum statistics. Simple analytical expressions can be derived for it in the zero-range and zero-temperature theory. In a homonuclear system of three identical bosons, $L_3^h(a)$ takes on the form of the well-known scaling law ($a < 0$) [5,27,34,95,96]

$$L_3^h(a) \propto \frac{\sinh(2\eta)}{\sin^2[s_0 \ln(a/a_-)] + \sinh^2\eta} a^4 \qquad (7)$$

that follows a general a^4 scaling and is modulated by a dimensionless log-periodic function, which contains the Efimov physics. Here, the position of an Efimov resonance a_- serves as the 3BP, and the inelasticity parameter η characterizes the probability of the trimer to decay into a deeply bound atom-dimer scattering channel. The behavior of the modulating function depends on the sign of a, and for $a < 0$ results in pronounced, log-periodic maxima at $a_-^{(n)}$, which are the Efimov resonances. The resonances are log-periodically separated with a period that corresponds to the scaling factor λ. Their origin can be understood intuitively in the hyperspherical picture [33], in which they arise because of three-body shape resonances behind a potential barrier [97]. Due to the complexity of accounting for all of the contributing molecular degrees of freedom at short particle separations, η is generally determined from experimental data [37]. In general, η may differ for positive and negative scattering length; however, they are assumed equal in the most simple analysis. In more complex situations or for very broad Feshbach resonances, a different or even magnetic field dependent η may be considered [98].

In stark contrast to the homonuclear case, where only a single scattering length is relevant, in heteronuclear systems two and, in general, three scattering lengths can be varied simultaneously. The scattering observables contain much richer signatures of Efimov physics, and can even give rise to novel phenomena, for example, simultaneous interference minima and resonant enhancement in atom-molecule collisions, without counterpart in the homonuclear Efimov scenario [75]. Nevertheless, microscopic processes giving rise to recombination resonances or interference minima are similar and do not significantly differ from the homonuclear ones.

Therefore, let us highlight this feature for the *BBX* system, where both scattering lengths a and $\bar{a}$ are large and negative. The full account of all the possible scaling laws for different relative magnitudes of a

and $\bar{a}$ is covered by [47,75,99]. In this case, the scaling law takes the form [75]

$$L_3(a,\bar{a}) \propto \begin{cases} \dfrac{\sinh(2\eta)}{\sin^2[s_0\ln(\bar{a}/\bar{a}_-)+s_0^*\ln(a/\bar{a})]+\sinh^2\eta}a^4 \\ \qquad\qquad \text{if } |a|\gg|\bar{a}|\,, \\ \dfrac{\sinh(2\eta)}{\sin^2[s_0\ln(a/a_-)]+\sinh^2\eta}a^2\bar{a}^2 \\ \qquad\qquad \text{if } |a|\ll|\bar{a}|\,, \end{cases} \tag{8}$$

where $\bar{a}_-$ and a_- are 3BPs, and s_0 and s_0^* characterize the scaling factors for two and three resonant interactions, respectively. The prefactor that determines the absolute magnitude of L_3 depends on the mass ratio in a non-trivial way [47]. Similarly, to the homonuclear case, if only one of the scattering lengths is varied the recombination spectrum contains a log-periodic modulation and necessarily undergoes a transition between $a^2\bar{a}^2$ and a^4 scaling, governed by the relative values of a and $\bar{a}$. Additionally, in realistic systems, where interactions are controlled via Feshbach resonances, typically both scattering lengths are tuned simultaneously in an non-independent, disproportionate way. This results in a series of recombination maxima that are only approximately log-periodically separated. Thus, even in the zero-range theory for realistic heteronuclear systems deviations from an ideal log-periodic scaling behavior in the form of Efimov-period-dependent scaling factors are expected. Such modifications to the universal Efimov scenario, where a and $\bar{a}$ are continuously tuned between arbitrary, finite values can be numerically treated with, for example, the S-matrix formalism [46,100,101], optical potentials [102], or full hyperspherical calculations [76].

The situation is notably more complicated for positive scattering lengths, in the regions $a > 0$ and/or $\bar{a} > 0$, since either intra- or interspecies universal dimer states can significantly contribute to the scattering dynamics. The system can be prepared in either the three-body or atom-dimer scattering channel, for each of which the experimental observables cardinally differ. Based on similar arguments as previously, the three-body recombination rates can be derived [5,34,75,78]. Also, here, a general scaling law is modulated by a strictly or approximately log-periodic function that can contain only minima, only maxima, or minima and maxima, depending on the relative magnitudes of individual scattering lengths. In contrast to recombination resonances, minima are created by two destructively interfering scattering pathways of three-atom and the universal atom-dimer channels, somewhat reminiscent of Stückelberg interferometry [103,104].

Unitarity limit

The observation of Efimovian features relies on the capability of tuning the collision properties by several orders of magnitude. While broad Feshbach resonances, in principle, can be used to realize infinitely attractive or repulsive interactions, the collisional cross sections are always limited by the thermal de Broglie wavelength. The three-body recombination rate at finite temperature is unitarity limited by [101]

$$L_3^{\lim} = \frac{4\pi^2\hbar^5}{\mu_3\,(k_B T)^2}, \tag{9}$$

where $\mu_3 = \sqrt{m_1 m_2 m_3/(m_1+m_2+m_3)}$ is the three-body reduced mass for the three particles with masses m_1, m_2, and m_3, and k_B is the Boltzmann constant. The loss rate from the trap cannot be faster than $L_3^{\lim}$, which limits the maximum achievable recombination rate and, consequently, the number of consecutive features that can be observed for a given temperature. This is also the reason why the recent experiments, in which the second sequential Efimov resonance [48] or three consecutive resonances [43,44] have been observed, have employed extremely low-temperatures or heteronuclear systems with drastically reduced scaling factors, respectively.

EXPERIMENTAL EVIDENCE IN ULTRACOLD QUANTUM GASES

Three-body recombination resonances

In a typical ultracold gas experiment, a small sample of atoms is cooled down by standard laser cooling techniques [94,105], and confined in an optical dipole trap [106]. Owing to the low-temperatures and optical pumping techniques, complete control over both internal and external degrees of freedom can be achieved. In this way, the ultracold ensemble of atoms and molecules can be prepared in well-defined magnetic spin states of corresponding hyperfine levels that represent a single scattering channel. The most straightforward approach to probe the Efimov scenario is atom-loss spectroscopy, identical to the one used for detecting Feshbach resonances [23]. The scattering length is tuned by scanning the magnetic field across a Feshbach resonance. Efimov resonances in atom-loss spectra emerge as additional modulations at the side of a large

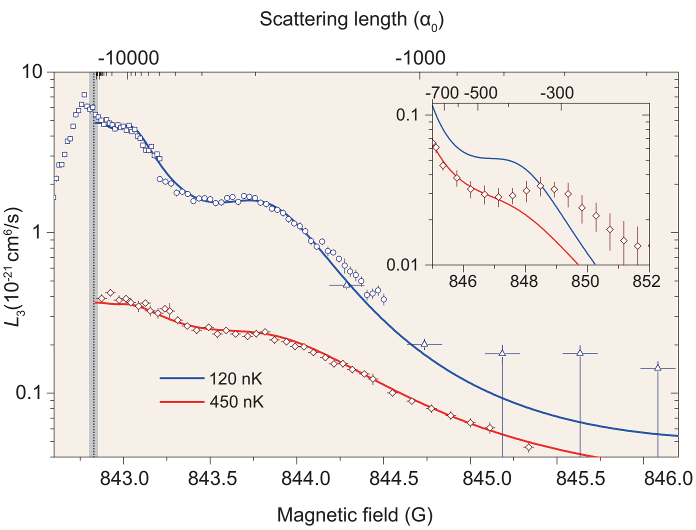

Figure 7. ^{6}Li-^{133}Cs-^{133}Cs three-body recombination event rate constant L_3 at a temperature of 450 nK (red diamonds) and at 120 nK (blue squares, circles, triangles), and fits to the zero-range theory. The pole of the Feshbach resonance and its uncertainty are indicated by the dotted line and the gray area, respectively. Three Efimov resonances are observed, which are located at ∼843.0, 843.8, and 848.9 G. The inset shows how the Efimov ground state resonance deviates from the zero-range theory. Reprinted from [46]. Copyright 2016 by the American Physical Society.

loss-feature that is associated with the Feshbach resonance.

While such spectra represent already strong hints for the existence of few-body resonances, and their positions can be approximately detected, it does not yield the exact composition of the number of particles undergoing a recombination or relaxation event. For this purpose, the time evolution of the atom number of each species in the mixture can be recorded, which is fitted with coupled rate equations that describe the composition of particles involved in the recombination. This yields loss-rate coefficients, which can be directly compared with theoretical predictions from Equations (7) and (8), or other appropriate cases [5,47,75,99].

Initial experiments on heteronuclear systems investigated ^{41}K-^{87}Rb mixtures via atom-loss measurements, where Rb-Rb-K and K-K-Rb three-body resonances were reported [40,41]. However, the positions of the resonances disagreed with estimates of the three-body parameter [76] and predictions for the available sample temperatures [107] [see also Equation (9)]. Subsequent recombination-rate experiments in the ^{40}K-^{87}Rb system [38,39] were not able to confirm the initial observation. The results on Efimov physics, in this mixture, are still inconclusive with more groups working in this direction [108].

A series of three consecutive Efimov resonances was observed for the first time in the ultracold mixture of fermionic ^{6}Li and bosonic ^{133}Cs atoms [43–46]. These measurements investigated atom-loss as well as three-body recombination rate spectra. The latter is shown in Fig. 7 as a function of the magnetic field and the interspecies scattering length. For the data taken at a lower temperature a third feature emerges, clearly demonstrating the second excited Efimov resonance and the importance of extending the window of universality by lowering the temperature. The comparison of experimentally determined event rate with the zero-range theory [101] recaptures the temperature dependence and the positions of the two excited three-body resonances, while the ground state deviates. This hints at non-universal effects due to van der Waals forces, since $a_-^{(0)} \sim -3r_{\rm vdW}^{\rm LiCs}$, and the departure from the window of universality at the short-range length scales. Already in homonuclear systems small deviations from universal zero-range theory have been observed for a ground-state Efimov triatomic resonance [109], where $a_-^{(0)} \sim -9r_{\rm vdW}$ [81,83]. Large deviations have been reported for atom-dimer Efimov resonances, see for example, [31,61,110,111].

Another approach has been employed to reveal the position of an Efimov resonance in the ^{7}Li-^{87}Rb system [42]. An atom undergoing a three-body recombination process and leaving the confinement removes less energy from the ensemble than its average [96,112,113]. The excess energy is redistributed and leads to heating of the sample. Since the recombination rate depends on the interspecies scattering length, the resulting increase in ensemble temperature can also be used to indirectly map out the positions of few-body resonances.

Atom-dimer resonances

Atom-dimer resonances are observed in ultracold atom-molecule collisions that undergo vibrational relaxation into deeply bound states and are expelled from the trap due to energy conservation. Analogous to three-body resonances, the magnetic field is tuned in order to vary the scattering length, and the analysis of recorded trap loss rates yields the relaxation rate constant for the particular interaction strength. Since this mechanism involves a bound dimer, it is realized if $a > 0$ or $\bar{a} > 0$.

Up to date heteronuclear atom-dimer resonances have been investigated with the ^{40}K^{87}Rb [38,39] and ^{41}K-^{87}Rb [40,41] mixtures. Atom-dimer relaxation rate spectra are shown in Fig. 8 for fermionic ^{40}K^{87}Rb Feshbach molecules and three different collision partners, namely, ferminoic ^{40}K atoms in two different spin states, and bosonic ^{87}Rb atoms [38]. A single, pronounced resonance is observed around $a_* = 230\, a_0$ for molecule collisions with Rb (cf. Fig. 3), while the scattering in other channels is

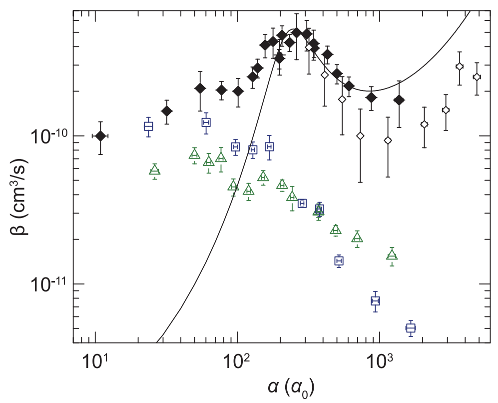

Figure 8. Atom-dimer relaxation rate coefficient β for collisions of $^{40}K^{87}Rb$ molecules with ^{40}K atoms in two different spin states (triangles and squares), and ^{87}Rb atoms at a temperature of 300 nK (solid diamonds) and 150 nK (open diamonds). An atom-dimer resonance is visible in the KRb-Rb scattering spectrum at $a \approx 230a_0$. Reprinted from [38]. Copyright 2013 by the American Physical Society.

suppressed by either Fermi statistics or the absence of a Feshbach resonance. There is good agreement with the zero-range theory for non-interacting bosons [47], which is used to extract the resonance position.

An alternative approach in probing the positions of atom-dimer crossing is to measure atom-loss features at the three-body threshold [40,41]. While such experiments are simpler because they do not require the preparation of molecule–atom mixtures, the connection between the observed signatures and a_* is problematic. Corresponding three-body recombination measurements [38,39] have not revealed equivalent features, thus, the interpretation of the initial atom-loss signal [40,41] is questionable. Further, experiments will be beneficial to settle the observed deviations from zero-range predictions and different behavior for various K isotopes [108].

CONCLUSION AND OUTLOOK

The heteronuclear Efimov scenario is becoming a new paradigm for studying universal physics, starting from few-body phenomena, and their relation to the individual constituents via non-universal corrections toward many-body systems and quasiparticle dynamics. Two significant differences in comparison to homonuclear systems can be identified: the first is the mass-imbalance, which yields different scaling factors and in special cases can simplify the theoretical treatment of the three-body problem. And the second is the additional, independent interaction parameter, which produces novel three-body phenomena with no counterexamples for the homonuclear case. While the mass-imbalance can be explored by choosing an appropriate combination of particles, independent tuning of interactions is more challenging. Potentially, two different kinds of scattering resonances could be used—magnetic ones, as done in most ultracold-atom experiments, and optically-[114–116] or rf-field- [117–120] induced ones. This would allow one to explore the entire spectrum of rich phenomena associated with the heteronuclear Efimov effect in a much more controlled way.

Close collaboration between theory and experiment has vastly extended our understanding of few-body physics and the heteronuclear Efimov effect. Various theoretical approaches that include the hyperspherical adiabatic framework [76], effective field theory [47,99], S-matrix formalism [100,101], or optical potentials [102] are rapidly gaining capabilities to quantitatively describe the three-body problem not only in idealized cases, but also for realistic experimental parameters, such as finite temperatures and overlapping Feshbach resonances. There are still a lot of open questions that concern the specific details of a particular Feshbach resonance, three-body forces and other microscopic interactions.

At the same time, a plethora of intriguing directions for further studies, reaching well beyond the classical heteronuclear Efimov scenario in three dimensions, are actively pursued experimentally and theoretically. A series of proposals make use of interactions stemming not from *s*-wave collisions but from higher partial waves [121–123]. Moreover, it has been suggested to tune the external degrees of freedom by confining the movement of three particles to two or one dimensions (see [124] for a recent overview). While for the homonuclear case in two dimensions two universal Efimov states are predicted, two more are expected in heteronuclear systems [125]. A combination of both, p-wave interaction and two-dimensional confinement, is summarized in the so-called super Efimov effect, showing a double exponential scaling in the trimer energy spectrum [126–128]. Further theoretical effort strives for the understanding of the Efimov effect with underlying pairwise dipole-dipole interactions [129,130]. Ultimately, by adding one like particle at a time four-, five- and higher order systems can be realized [131–135] and insights into few-body correlations and their link to emergent many-body phenomena can be investigated [136,137]. All these and many more excellent proposals provide one with an exceptionally rich playground for exploring few-body physics that are not only limited to three particles and isotropic interactions. We are confident that this is only the beginning of a journey in the realm of ultracold few-body physics, and the further years will bring a lot of insight and excitement.

ACKNOWLEDGEMENTS

The authors would like to thank the collaborations and discussions with J. Bohn, J. D´Incao, F. Ferlaino, C. Greene, R. Grimm, S. Jochim, P. Julienne, S. Knoop, D. Petrov, R. Pires, M. Repp, B. Ruzic, C. Salomon, T. Tiecke, E. Tiemann, L. Wacker, J. Wang, Y. Wang, F. Werner, S. Whitlock, N. Zinner, and G. Zürn at various stages during this work.

FUNDING

This work is supported in part by the Heidelberg Center for Quantum Dynamics, IMPRS-QD, DAAD and Baden-Württemberg Stiftung.

REFERENCES

1. Efimov V. Energy levels arising from resonant two-body forces in a three-body system. *Phys Lett B* 1970; **33**: 563–4.
2. Efimov V. Energy levels of three resonantly interacting particles. *Nucl Phys A* 1973; **210**: 157–88.
3. Efimov V. Low-energy properties of three resonantly interacting particles. *Sov J Nucl Phys* 1979; **29**: 546.
4. Nielsen E, Fedorov D and Jensen A *et al.* The three-body problem with short-range interactions. *Phys Rep* 2001; **347**: 373–459.
5. Braaten E and Hammer HW. Universality in few-body systems with large scattering length. *Phys Rep* 2006; **428**: 259–390.
6. Hammer HW and Platter L. Efimov states in nuclear and particle physics. *Annu Rev Nucl Part Sci* 2010; **60**: 207–36.
7. Zinner NT and Jensen AS. Comparing and contrasting nuclei and cold atomic gases. *J Phys G* 2013; **40**: 053101.
8. Lim TK, Duffy SK and Damer WC. Efimov state in the ^{4}He trimer. *Phys Rev Lett* 1977; **38**: 341–3.
9. Nielsen E, Fedorov DV and Jensen AS. The structure of the atomic helium trimers: halos and Efimov states. *J Phys B* 1998; **31**: 4085–105.
10. Cencek W, Przybytek M and Komasa J *et al.* Effects of adiabatic, relativistic, and quantum electrodynamics interactions on the pair potential and thermophysical properties of helium. *J Chem Phys* 2012; **136**: 224303.
11. Kunitski M, Zeller S and Voigtsberger J *et al.* Observation of the Efimov state of the helium trimer. *Science* 2015; **348**: 551–5.
12. Hiyama E and Kamimura M. Universality in Efimov-associated tetramers in ^{4}He. *Phys Rev A* 2014; **90**: 052514.
13. Hansen PG, Jensen AS and Jonson B. Nuclear halos. *Annu Rev Nucl Sci* 1995; **45**: 591–634.
14. Jensen AS, Riisager K and Fedorov DV *et al.* Structure and reactions of quantum halos. *Rev Mod Phys* 2004; **76**: 215–61.
15. Frederico T, Delfino A and Tomio L *et al.* Universal aspects of light halo nuclei. *Prog Part Nucl Phys* 2012; **67**: 939.
16. Riisager K. Halos and related structures. *Phys Scr* 2013; **2013**: 014001.
17. Carlson J and Schiavilla R. Structure and dynamics of few-nucleon systems. *Rev Mod Phys* 1998; **70**: 743–841.
18. Fedorov DV, Jensen AS and Riisager K. Efimov states in halo nuclei. *Phys Rev Lett* 1994; **73**: 2817–20.
19. Acharya B, Ji C and Phillips D. Implications of a matter-radius measurement for the structure of carbon-22. *Phys Lett B* 2013; **723**: 196–200.
20. Tanaka K, Yamaguchi T and Suzuki T *et al.* Observation of a large reaction cross section in the drip-line nucleus 22C. *Phys Rev Lett* 2010; **104**: 062701.
21. Hagen G, Hagen P and Hammer HW *et al.* Efimov physics around the neutron-rich ^{60}Ca isotope. *Phys Rev Lett* 2013; **111**: 132501.
22. Kemper KW and Cottle PD. Viewpoint: a breakthrough observation for neutron dripline physics. *Physics* 2010; **3**: 13.
23. Chin C, Grimm R and Julienne PS *et al.* Feshbach resonances in ultracold gases. *Rev Mod Phys* 2010; **82**: 1225–86.
24. Köhler T, Góral K and Julienne PS. Production of cold molecules via magnetically tunable Feshbach resonances. *Rev Mod Phys* 2006; **78**: 1311–61.
25. Kraemer T, Mark M and Waldburger P *et al.* Evidence for Efimov quantum states in an ultracold gas of caesium atoms. *Nature* 2006; **440**: 315–8.
26. Esry BD, Greene CH and Burke JP. Recombination of three atoms in the ultracold limit. *Phys Rev Lett* 1999; **83**: 1751–4.
27. Nielsen E and Macek JH. Low-energy recombination of identical bosons by three-body collisions. *Phys Rev Lett* 1999; **83**: 1566.
28. Bedaque PF, Braaten E and Hammer HW. Three-body recombination in Bose gases with large scattering length. *Phys Rev Lett* 2000; **85**: 908–11.
29. Lompe T, Ottenstein TB and Serwane F *et al.* Radio-frequency association of Efimov trimers. *Science* 2010; **330**: 940–4.
30. Nakajima S, Horikoshi M and Mukaiyama T *et al.* Measurement of an Efimov trimer binding energy in a three-component mixture of ^{6}Li. *Phys Rev Lett* 2011; **106**: 143201.
31. Machtey O, Shotan Z and Gross N *et al.* Association of Efimov trimers from a three-atom continuum. *Phys Rev Lett* 2012; **108**: 210406.
32. Braaten E and Hammer HW. Efimov physics in cold atoms. *Ann Phys* 2007; **322**: 120–63.
33. Greene CH. Universal insights from few-body land. *Phys Today* 2010; **63**: 40.
34. Ferlaino F, Zenesini A and Berninger M *et al.* Efimov resonances in ultracold quantum gases. *Few-Body Syst* 2011; **51**: 113–33.
35. Blume D. Few-body physics with ultracold atomic and molecular systems in traps. *Rep Prog Phys* 2012; **75**: 046401.
36. Wang Y, D'Incao JP and Esry BD. Ultracold few-body systems. In: Arimondo E, Berman PR and Lin CC (eds). *Advances in Atomic, Molecular, and Optical Physics*. Amsterdam: Academic Press, 2013, 1–115.
37. Wang Y, Julienne P and Greene CH. Few-body physics of ultracold atoms and molecules with long-range interactions. In: Madison KW, Bongs K and Carr LD *et al.* (eds). *Annual Review of Cold Atoms and Molecules*. Singapore: World Scientific Publishing, 2015, 77–134.

38. Bloom RS, Hu MG and Cumby TD *et al.* Tests of universal three-body physics in an ultracold Bose-Fermi mixture. *Phys Rev Lett* 2013; **111**: 105301.
39. Hu MG, Bloom RS and Jin DS *et al.* Avalanche-mechanism loss at an atom-molecule Efimov resonance. *Phys Rev A* 2014; **90**: 013619.
40. Barontini G, Weber C and Rabatti F *et al.* Observation of heteronuclear atomic Efimov resonances. *Phys Rev Lett* 2009; **103**: 043201.
41. Barontini G, Weber C and Rabatti F *et al.* Erratum: observation of heteronuclear atomic Efimov resonances [*Phys. Rev. Lett.* 103, 043201 (2009)]. *Phys Rev Lett* 2010; **104**: 059901(E).
42. Maier RAW, Eisele M and Tiemann E *et al.* Efimov resonance and three-body parameter in a lithium-rubidium mixture. *Phys Rev Lett* 2015; **115**: 043201.
43. Pires R, Ulmanis J and Häfner S *et al.* Observation of Efimov resonances in a mixture with extreme mass imbalance. *Phys Rev Lett* 2014; **112**: 250404.
44. Tung SK, Jiménez-García K and Johansen J *et al.* Geometric scaling of Efimov states in a ^{6}Li-^{133}Cs mixture. *Phys Rev Lett* 2014; **113**: 240402.
45. Ulmanis J, Häfner S and Pires R *et al.* Universality of weakly bound dimers and Efimov trimers close to LiCs Feshbach resonances. *New J Phys* 2015; **17**: 055009.
46. Ulmanis J, Häfner S and Pires R *et al.* Universal three-body recombination and Efimov resonances in an ultracold Li-Cs mixture. *Phys Rev A* 2016; **93**: 022707.
47. Helfrich K, Hammer HW and Petrov DS. Three-body problem in heteronuclear mixtures with resonant interspecies interaction. *Phys Rev A* 2010; **81**: 042715.
48. Huang B, Sidorenkov LA and Grimm R *et al.* Observation of the second triatomic resonance in Efimov's scenario. *Phys Rev Lett* 2014; **112**: 190401.
49. Frederico T, Delfino A and Hadizadeh M *et al.* Universality in four-boson systems. *Few-Body Syst* 2013; **54**: 559–68.
50. Derevianko A, Babb JF and Dalgarno A. High-precision calculations of van der Waals coefficients for heteronuclear alkali-metal dimers. *Phys Rev A* 2001; **63**: 052704.
51. Sakurai JJ and Napolitano JJ. *Modern Quantum Mechanics*. San Francisco: Addison-Wesley, 2011.
52. Porsev SG and Derevianko A. Accurate relativistic many-body calculations of van der waals coefficients C_8 and C_{10} for alkali-metal dimers. *J Chem Phys* 2003; **119**: 844.
53. Porsev SG, Safronova MS and Derevianko A *et al.* Relativistic many-body calculations of van der Waals coefficients for Yb-Li and Yb-Rb dimers. *Phys Rev A* 2014; **89**: 022703.
54. Jones KM, Tiesinga E and Lett PD *et al.* Ultracold photoassociation spectroscopy: long-range molecules and atomic scattering. *Rev Mod Phys* 2006; **78**: 483–535.
55. Berninger M, Zenesini A and Huang B *et al.* Feshbach resonances, weakly bound molecular states, and coupled-channel potentials for cesium at high magnetic fields. *Phys Rev A* 2013; **87**: 032517.
56. Moerdijk AJ, Verhaar BJ and Axelsson A. Resonances in ultracold collisions of ^{6}Li, ^{7}Li, and ^{23}Na. *Phys Rev A* 1995; **51**: 4852–61.
57. Pires R, Repp M and Ulmanis J *et al.* Analyzing Feshbach resonances: A ^{6}Li-^{133}Cs case study. *Phys Rev A* 2014; **90**: 012710.
58. Dieckmann K, Stan CA and Gupta S *et al.* Decay of an ultracold fermionic lithium gas near a Feshbach resonance. *Phys Rev Lett* 2002; **89**: 203201.
59. Bourdel T, Cubizolles J and Khaykovich L *et al.* Measurement of the interaction energy near a Feshbach resonance in a ^{6}Li Fermi gas. *Phys Rev Lett* 2003; **91**: 020402.
60. Weber C, Barontini G and Catani J *et al.* Association of ultracold double-species bosonic molecules. *Phys Rev A* 2008; **78**: 061601.
61. Machtey O, Kessler DA and Khaykovich L. Universal dimer in a collisionally opaque medium: experimental observables and Efimov resonances. *Phys Rev Lett* 2012; **108**: 130403.
62. Zhang S and Ho TL. Atom loss maximum in ultra-cold Fermi gases. *New J Phys* 2011; **13**: 055003.
63. Khramov AY, Hansen AH and Jamison AO *et al.* Dynamics of Feshbach molecules in an ultracold three-component mixture. *Phys Rev A* 2012; **86**: 032705.
64. Bartenstein M, Altmeyer A and Riedl S *et al.* Precise determination of ^{6}Li cold collision parameters by radio-frequency spectroscopy on weakly bound molecules. *Phys Rev Lett* 2005; **94**: 103201.
65. Gribakin GF and Flambaum VV. Calculation of the scattering length in atomic collisions using the semiclassical approximation. *Phys Rev A* 1993; **48**: 546–53.
66. Landau LD and Lifshitz EM. *Quantum Mechanics: Non-Relativistic Theory*. New York: Pergamon Press, 1991.
67. Coon SA and Holstein BR. Anomalies in quantum mechanics: the $1/r^2$ potential. *Am J Phys* 2002; **70**: 513.
68. Essin AM and Griffiths DJ. Quantum mechanics of the $1/x^2$ potential. *Am J Phys* 2006; **74**: 109.
69. Amado RD and Noble JV. Efimov's effect: a new pathology of three-particle systems. II. *Phys Rev D* 1972; **5**: 1992.
70. Efimov V. Weakly bound states of three resonantly-interacting particles. *Sov J Nuc Phys* 1971; **12**: 589.
71. D'Incao JP and Esry BD. Enhancing the observability of the Efimov effect in ultracold atomic gas mixtures. *Phys Rev A* 2006; **73**: 030703.
72. Fedorov DV and Jensen AS. Efimov effect in coordinate space Faddeev equations. *Phys Rev Lett* 1993; **71**: 4103–6.
73. Fonseca AC, Redish EF and Shanley P. Efimov effect in an analytically solvable model. *Nucl Phys A* 1979; **320**: 273–88.
74. Petrov D. The Few-atom problem. In: Salomon C, Shlyapnikov GV and Cugliandolo LF (eds). *Many-Body Physics with Ultracold Gases: Lecture Notes of the Les Houches Summer School*. Oxford: Oxford University Press, 2010, 109–160.
75. D'Incao JP and Esry BD. Ultracold three-body collisions near overlapping Feshbach resonances. *Phys Rev Lett* 2009; **103**: 083202.
76. Wang Y, Wang J and D'Incao JP *et al.* Universal three-body parameter in heteronuclear atomic systems. *Phys Rev Lett* 2012; **109**: 243201.
77. Thomas LH. The interaction between a neutron and a proton and the structure of H^3. *Phys Rev* 1935; **47**: 903–9.
78. D'Incao JP, Greene CH and Esry BD. The short-range three-body phase and other issues impacting the observation of Efimov physics in ultracold quantum gases. *J Phys B* 2009; **42**: 044016.
79. Hammer HW, Nogga A and Schwenk A. Colloquium: Three-body forces: from cold atoms to nuclei. *Rev Mod Phys* 2013; **85**: 197–217.
80. Gross N, Shotan Z and Kokkelmans S *et al.* Nuclear-spin-independent short-range three-body physics in ultracold atoms. *Phys Rev Lett* 2010; **105**: 103203.
81. Berninger M, Zenesini A and Huang B *et al.* Universality of the three-body parameter for Efimov states in ultracold cesium. *Phys Rev Lett* 2011; **107**: 120401.
82. Wild RJ, Makotyn P and Pino JM *et al.* Measurements of Tan's contact in an atomic Bose-Einstein condensate. *Phys Rev Lett* 2012; **108**: 145305.
83. Wang J, D'Incao JP and Esry BD *et al.* Origin of the three-body parameter universality in Efimov physics. *Phys Rev Lett* 2012; **108**: 263001.
84. Naidon P, Endo S and Ueda M. Physical origin of the universal three-body parameter in atomic Efimov physics. *Phys Rev A* 2014; **90**: 022106.
85. Naidon P, Endo S and Ueda M. Microscopic origin and universality classes of the Efimov three-body parameter. *Phys Rev Lett* 2014; **112**: 105301.
86. Wang Y and Julienne PS. Universal van der Waals physics for three cold atoms near Feshbach resonances. *Nat Phys* 2014; **10**: 768773.

87. Lee MD, Köhler T and Julienne PS. Excited Thomas-Efimov levels in ultracold gases. *Phys Rev A* 2007; **76**: 012720.
88. Jona-Lasinio M and Pricoupenko L. Three resonant ultracold bosons: off-resonance effects. *Phys Rev Lett* 2010; **104**: 023201.
89. Ji C, Phillips DR and Platter L. Beyond universality in three-body recombination: an effective field theory treatment. *Eur Phys L* 2010; **92**: 13003.
90. Schmidt R, Rath S and Zwerger W. Efimov physics beyond universality. *Eur Phys J B* 2012; **85**: 1.
91. Sørensen PK, Fedorov DV and Jensen AS *et al.* Finite-range effects in energies and recombination rates of three identical bosons. *J Phys B* 2013; **46**: 075301.
92. Ji C, Braaten E and Phillips DR *et al.* Universal relations for range corrections to Efimov features. *Phys Rev A* 2015; **92**: 030702.
93. Kievsky A and Gattobigio M. Universal range corrections to Efimov trimers for a class of paths to the unitary limit. *Phys Rev A* 2015; **92**: 062715.
94. Inguscio M, Stringari S and Wieman CE (eds). *Proceedings of the International School of Physics 'Enrico Fermi', Course CXL, Bose-Einstein Condensation in Atomic Gases*. Amsterdam: IOS Press, 1999.
95. Fedichev PO, Reynolds MW and Shlyapnikov GV. Three-body recombination of ultracold atoms to a weakly bound *s* level. *Phys Rev Lett* 1996; **77**: 2921–4.
96. Weber T, Herbig J and Mark M *et al.* Three-body recombination at large scattering lengths in an ultracold atomic gas. *Phys Rev Lett* 2003; **91**: 123201.
97. Esry BD and D'Incao JP. Efimov physics in ultracold three-body collisions. *J Phys Conf Ser* 2007; **88**: 012040.
98. Wenz AN, Lompe T and Ottenstein TB *et al.* Universal trimer in a three-component Fermi gas. *Phys Rev A* 2009; **80**: 040702.
99. Helfrich K and Hammer HW. The heteronuclear Efimov effect. *EPJ Web of Conferences* 2009; **3**: 02007.
100. Rem BS, Grier AT and Ferrier-Barbut I *et al.* Lifetime of the Bose gas with resonant interactions. *Phys Rev Lett* 2013; **110**: 163202.
101. Petrov DS and Werner F. Three-body recombination in heteronuclear mixtures at finite temperature. *Phys Rev A* 2015; **92**: 022704.
102. Mikkelsen M, Jensen AS and Fedorov DV *et al.* Three-body recombination of two-component cold atomic gases into deep dimers in an optical model. *J Phys B* 2015; **48**: 085301.
103. Stückelberg ECG. Theorie der unelastischen Stösse zwischen Atomen. *Helv Phys Acta* 1932; **5**: 369.
104. Mark M, Kraemer T and Waldburger P *et al.* 'Stückelberg interferometry' with ultracold molecules. *Phys Rev Lett* 2007; **99**: 113201.
105. Inguscio M, Ketterle W and Salomon C (eds). *Proceedings of the International School of Physics 'Enrico Fermi', Course CLXIV, Ultra-Cold Fermi Gases*. Amsterdam: IOS Press, 2007.
106. Grimm R, Weidemüller M and Ovchinnikov YB. Optical dipole traps for neutral atoms. In: Bederson B and Walther H (eds). *Advances in Atomic, Molecular, and Optical Physics.* Amsterdam: Academic Press, 2000, 95–170.
107. D'Incao JP, Suno H and Esry BD. Limits on universality in ultracold three-boson recombination. *Phys Rev Lett* 2004; **93**: 123201.
108. (a) Wacker L, Jørgensen NB and Birkmose D *et al.* Tunable dual-species Bose-Einstein condensates of ^{39}K and ^{87}Rb. *Phys Rev A* 2015; **92**: 053602.
 (b) Wacker LJ, Jørgensen NB and Birkmose D *et al.* Absence of observable Efimov resonances in ultracold KRb mixtures. 2016, arXiv:1604.03693.
109. Huang B, Sidorenkov LA and Grimm R. Finite-temperature effects on a triatomic Efimov resonance in ultracold cesium. *Phys Rev A* 2015; **91**: 063622.
110. Knoop S, Ferlaino F and Mark M *et al.* Observation of an Efimov-like trimer resonance in ultracold atom-dimer scattering. *Nat Phys* 2009; **5**: 227–30.
111. Zenesini A, Huang B and Berninger M *et al.* Resonant atom-dimer collisions in cesium: testing universality at positive scattering lengths. *Phys Rev A* 2014; **90**: 022704.
112. Ottenstein TB, Lompe T and Kohnen M *et al.* Collisional stability of a three-component degenerate Fermi gas. *Phys Rev Lett* 2008; **101**: 203202.
113. Roy S, Landini M and Trenkwalder A *et al.* Test of the universality of the three-body Efimov parameter at narrow Feshbach resonances. *Phys Rev Lett* 2013; **111**: 053202.
114. Bohn JL and Julienne PS. Prospects for influencing scattering lengths with far-off-resonant light. *Phys Rev A* 1997; **56**: 1486–91.
115. Bohn JL and Julienne PS. Semianalytic theory of laser-assisted resonant cold collisions. *Phys Rev A* 1999; **60**: 414–25.
116. Borkowski M, Ciuryło R and Julienne PS *et al.* Line shapes of optical Feshbach resonances near the intercombination transition of bosonic ytterbium. *Phys Rev A* 2009; **80**: 012715.
117. Kaufman AM, Anderson RP and Hanna TM *et al.* Radio-frequency dressing of multiple Feshbach resonances. *Phys Rev A* 2009; **80**: 050701.
118. Tscherbul TV, Calarco T and Lesanovsky I *et al.* Rf-field-induced Feshbach resonances. *Phys Rev A* 2010; **81**: 050701.
119. Hanna TM, Tiesinga E and Julienne PS. Creation and manipulation of Feshbach resonances with radiofrequency radiation. *New J Phys* 2010; **12**: 083031.
120. Xie T, Wang GR and Huang Y *et al.* The radio frequency field modulation of magnetically induced heteronuclear Feshbach resonance. *J Phys B* 2012; **45**: 145302.
121. Helfrich K and Hammer HW. On the Efimov effect in higher partial waves. *J Phys B: At Mol Opt Phys* 2011; **44**: 215301
122. Marcelis B, Kokkelmans SJJMF and Shlyapnikov GV *et al.* Collisional properties of weakly bound heteronuclear dimers. *Phys Rev A* 2008; **77**: 032707.
123. Wang J, D'Incao JP and Wang Y *et al.* Universal three-body recombination via resonant *d*-wave interactions. *Phys Rev A* 2012; **86**: 062511.
124. D'Incao JP, Anis F and Esry BD. Ultracold three-body recombination in two dimensions. *Phys Rev A* 2015; **91**: 062710.
125. Levinsen J, Massignan P and Parish MM. Efimov trimers under strong confinement. *Phys Rev X* 2014; **4**: 031020.
126. Moroz S and Nishida Y. Super Efimov effect for mass-imbalanced systems. *Phys Rev A* 2014; **90**: 063631.
127. Nishida Y, Moroz S and Son DT. Super Efimov effect of resonantly interacting fermions in two dimensions. *Phys Rev Lett* 2013; **110**: 235301.
128. Volosniev AG, Fedorov DV and Jensen AS *et al.* Borromean ground state of fermions in two dimensions. *J Phys B* 2014; **47**: 185302.
129. Wang Y, D'Incao JP and Greene CH. Universal three-body physics for fermionic dipoles. *Phys Rev Lett* 2011; **107**: 233201.
130. Wang Y, D'Incao JP and Greene CH. Efimov effect for three interacting bosonic dipoles. *Phys Rev Lett* 2011; **106**: 233201.
131. Wang Y, Laing WB and von Stecher J *et al.* Efimov physics in heteronuclear four-body systems. *Phys Rev Lett* 2012; **108**: 073201.
132. Hammer HW and Platter L. Universal properties of the four-body system with large scattering length. *Eur Phys J A* 2007; **32**: 113–20.
133. von Stecher J, D'Incao JP and Greene CH. Signatures of universal four-body phenomena and their relation to the Efimov effect. *Nat Phys* 2009; **5**: 417–21.
134. von Stecher J. Weakly bound cluster states of Efimov character. *J Phys B* 2010; **43**: 101002.
135. Blume D and Yan Y. Generalized Efimov scenario for heavy-light mixtures. *Phys Rev Lett* 2014; **113**: 213201.
136. Levinsen J, Parish MM and Bruun GM. Impurity in a Bose-Einstein condensate and the Efimov effect. *Phys Rev Lett* 2015; **115**: 125302.
137. Ardila LAP and Giorgini S. Impurity in a Bose-Einstein condensate: study of the attractive and repulsive branch using quantum Monte Carlo methods. *Phys Rev A* 2015; **92**: 033612.